plexing filters with arbitrary amplitude and delay response," *1976 IEEE MTT-S Int. Microwave Symp. Digest*, IEEE Cat. no. 76CH1087-6MTT, pp. 116–118.
[3] M. H. Chen, F. Assal, and C. Mahle, "A contiguous band multiplexer," *Comsat Tech. Rev.*, vol. 6, no. 2, pp. 285–305, Fall 1976.
[4] J. D. Rhodes, "Direct design of symmetrical interacting bandpass channel diplexers," *Inst. Elec. Eng. Microwaves, Opt., Acoust.*, vol. 1, no. 1, pp. 34–40, Sept. 1976.
[5] R. Levy, "Filters with single transmission zeros at real or imaginary frequencies," *IEEE Trans. Microwave Theory Tech.*, vol. MTT-24, pp. 172–181, Apr. 1976.
[6] A. E. Atia, "Computer-aided design of waveguide mutiplexers," *IEEE Trans. Microwave Theory Tech.*, vol. MTT-22, pp. 332–336, Mar. 1974.
[7] N. Marcuvitz Ed., *Waveguide Handbook*. M.I.T. Radiation Lab. Series, vol. 10. New York: McGraw-Hill, 1951.
[8] S. B. Cohn, "Direct-coupled-resonator filters," *Proc. IRE*, vol 45, pp. 187–196, Feb. 1957.
[9] R. Levy, "Theory of direct-coupled-cavity filters," *IEEE Trans. Microwave Theory Tech.*, vol. MTT-15, pp. 340–348, June 1967.

Tables for Nonminimum-Phase Even-Degree Low-Pass Prototype Networks for the Design of Microwave Linear-Phase Filters

J. H. CLOETE, MEMBER, IEEE

Abstract*—The element values of a selection of even-degree nonminimum-phase low-pass prototype networks with equiripple passband amplitude and constant group delay in the least squares sense over a large percentage of the passband are tabulated. All the prototypes have passband insertion loss ripple $R=0.01$ dB and cutoff frequency $\omega_c=1.0$ rad/s at the 0.01-dB point. Five tables contain the element values of networks up to degree $N=20$. The tables are classified according to the number of transmission zeros at infinite frequency NZ_∞ and the passband frequency to which the group delay is constant in the least squares sense ω_d. The following combinations of NZ_∞ and ω_d are tabulated: $NZ_\infty=2$ and $\omega_d=0.9$; $NZ_\infty=4$ and $\omega_d=0.8$; $NZ_\infty=6$ and $\omega_d=0.7$; $NZ_\infty=8$ and $\omega_d=0.6$; and $NZ_\infty=10$ and $\omega_d=0.5$. The maximum phase and delay errors for each network are tabulated. Plots of the passband group delay and stopband insertion loss versus frequency, for each network, accompany the tables to facilitate selection of a prototype. The prototypes are suitable for the design of narrow-band generalized interdigital, generalized direct-coupled cavity waveguide, and generalized combline linear-phase filters. A simple algorithm for the analysis of the prototypes is given.

I. Introduction

THE SYMMETRICAL nonminimum-phase low-pass prototype network introduced by Rhodes [1] is shown for the even-degree case. It is topologically suited to the design of microwave bandpass filters capable of good amplitude selectivity while approximating closely to linear phase over a large percentage of the passband. The microwave filters are realized by providing coupling between nonadjacent resonators. Examples include the generalized interdigital filter [2], the generalized direct-coupled cavity waveguide filter [3]–[5] and the generalized combline filter [6].

Manuscript received February 13, 1978; revised June 27, 1978.
The author was with the Department of Electrical Engineering, University of Stellenbosch, Stellenbosch 7600, South Africa, on leave from the National Institute for Aeronautics and Systems Technology, Council for Scientific and Industrial Research, P.O. Box 395, Pretoria 0001, South Africa.

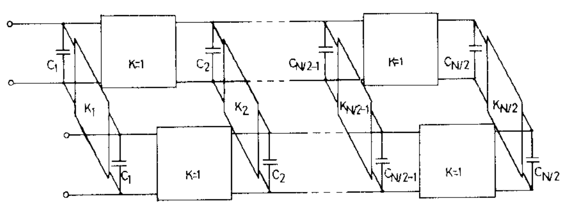

Fig. 1. The symmetrical even-degree nonminimum phase low-pass prototype network consisting of lumped capacitors and ideal admittance inverters. The notation for the network elements is consistent with the notation used in Tables I–V.

The first step in the design of a narrow-band microwave linear-phase filter is to find the element values of a low-pass prototype which satisfies the amplitude and phase or group delay specifications. When this step is completed the elements in the equivalent circuit of the microwave filter may be calculated [2], [3]. A number of approximation theories and techniques have been described for the construction of nonminimum-phase low-pass transfer functions from which the element values of the prototype networks can be synthesized [1], [4], [7]–[10]. These methods generally require considerable computation to achieve a satisfactory prototype. The method of Levy [4], applicable when only one pair of finite zeros provides

TABLE I
ELEMENT VALUES FOR LOW-PASS PROTOTYPE
$R=0.01$, $\omega_c=1.0$, $NZ_\infty=2$, $\omega_d=0.9$

R = 0.01 db ω_c = 1.0 rad/sec NZ_∞ = 2 ω_d = 0.9 rad/sec									
N	4	6	8	10	12	14	16	18	20
C1	0.685115	0.753304	0.782136	0.797192	0.807752	0.815966	0.821179	0.824991	0.828059
K1	0.171899	0.064565	0.033982	0.022164	0.011750	0.004081	0.001770	0.000633	0.000201
C2	1.154307	1.297451	1.360047	1.391675	1.413221	1.429582	1.439661	1.446886	1.452613
K2	0.818960	0.281599	0.134662	0.079645	0.045321	0.019800	0.009451	0.004107	0.001550
C3		1.777872	1.732142	1.759245	1.785200	1.807871	1.822790	1.833390	1.841616
K3		0.770867	0.375958	0.217576	0.132360	0.072683	0.039139	0.019972	0.008816
C4			2.066181	1.779143	1.730143	1.727850	1.737775	1.748043	1.756920
K4			0.608249	0.350911	0.232597	0.152014	0.095275	0.056647	0.029416
C5				2.800655	2.185692	2.021880	1.978869	1.972029	1.976647
K5				0.582255	0.370820	0.274870	0.200210	0.138688	0.086371
C6					2.969669	2.182479	1.953253	1.865856	1.832988
K6					0.470146	0.319480	0.251716	0.200015	0.150294
C7						3.662809	2.628839	2.291117	2.133668
K7						0.472260	0.322923	0.266721	0.229069
C8							3.663890	2.584902	2.209821
K8							0.391153	0.267807	0.229060
C9								4.380276	3.040882
K9								0.397245	0.270761
C10									4.254919
K10									0.337879
Average delay(sec)	2.28	4.70	7.35	10.13	12.95	15.74	18.58	21.44	24.28
Delay error(sec)	<0.05	<0.05	<0.05	<0.05	<0.05	<0.1	<0.1	<0.1	<0.2
Phase error(deg)	<0.2	<0.2	<0.2	<0.2	<0.2	<0.2	<0.2	<0.3	<1.0

TABLE II
ELEMENT VALUES FOR LOW-PASS PROTOTYPE
$R=0.01$, $\omega_c=1.0$, $NZ_\infty=4$, $\omega_d=0.8$

R = 0.01 db ω_c = 1.0 rad/sec NZ_∞ = 4 ω_d = 0.8 rad/sec								
N	6	8	10	12	14	16	18	20
C1	0.767954	0.791870	0.805281	0.813046	0.819328	0.823501	0.826887	0.829479
K1	0.000000	0.000000	0.000000	0.000000	0.000000	0.000000	0.000000	0.000000
C2	1.329865	1.381313	1.408724	1.424058	1.436201	1.444119	1.450452	1.455245
K2	0.197329	0.070040	0.028976	0.015973	0.006093	0.003018	0.001060	0.000362
C3	1.704204	1.735720	1.775454	1.799216	1.817667	1.829431	1.838585	1.845351
K3	0.869212	0.352026	0.163076	0.087439	0.041109	0.020430	0.008940	0.003597
C4		1.916714	1.728809	1.720559	1.731626	1.743469	1.753530	1.761040
K4		0.673675	0.366668	0.216595	0.123316	0.069430	0.035216	0.016502
C5			2.590631	2.098243	1.987945	1.969943	1.972916	1.980490
K5			0.651010	0.402827	0.275898	0.182013	0.110283	0.061253
C6				2.832099	2.096892	1.904724	1.841006	1 826061
K6				0 514866	0 348331	0.263398	0.193220	0 129795
C7					3.548571	2.543591	2.217715	2 089582
K7					0.506789	0 350916	0.287883	0.231071
C8						3.577886	2.508454	2 136427
K8						0.412378	0.291404	0.250745
C9							4.273132	2.964809
K9							0.415741	0.292130
C10								4.154701
K10								0.350514
Average delay(sec)	4.46	7.10	9.84	12 68	15.48	18.32	21.14	23.95
Delay error(sec)	<0.1	<0.05	<0.05	<0.05	<0.05	<0.05	<0.05	<0.1
Phase error(deg)	<0.5	<0.2	<0.1	<0.2	<0.1	<0.1	<0.1	<0.3

TABLE III
ELEMENT VALUES FOR LOW-PASS PROTOTYPE
$R=0.01$, $\omega_c=1.0$, $NZ_\infty=6$, $\omega_d=0.7$

R = 0.01 db ω_c = 1.0 rad/sec NZ_∞ = 6 ω_d = 0.7 rad/sec							
N	8	10	12	14	16	18	20
C1	0.800197	0.810713	0.817806	0.822437	0.826114	0.828678	0.830854
K1	0.000000	0.000000	0.000000	0.000000	0.000000	0.000000	0.000000
C2	1.398869	1.419688	1.433387	1.442156	1.449037	1.453778	1.457772
K2	0.000000	0.000000	0.000000	0.000000	0.000000	0.000000	0.000000
C3	1.758512	1.792463	1.813654	1.826672	1.836631	1.843327	1.848877
K3	0.253717	0.088573	0.031390	0.014260	0.005571	0.002752	0.000925
C4	1.752839	1.708460	1.725217	1.739896	1.751308	1.758829	1.764924
K4	0.767532	0.349748	0.161320	0.076702	0.034008	0.016613	0.007007
C5		2.341914	2.002279	1.965773	1.969223	1.977459	1.985173
K5		0.719023	0.424472	0.250659	0.134831	0.073345	0.035811
C6			2.573544	1.980303	1.849199	1.825952	1.824818
K6			0.576986	0.379388	0.262833	0.166653	0.097822
C7				3.343179	2.386541	2.132841	2.053304
K7				0.558178	0.393510	0.301335	0.216658
C8					3.411921	2.379979	2.042496
K8					0.452796	0.325169	0.271374
C9						4.119225	2.837710
K9						0.446750	0.325935
C10							4.034763
K10							0.371292
Average delay(sec)	6.69	9.48	12.26	15.09	17.88	20.71	23.51
Delay error(sec)	<0.2	<0.1	<0.1	<0.05	<0.1	<0.1	<0.1
Phase error(deg)	<0.5	<0.2	<0.1	<0.1	<0.2	<0.3	<0.3

adequate improvement of the delay (or stopband amplitude) is the exception.

The purpose of this paper is to circumvent, where possible, the computational effort implicit in the search for a suitable low-pass prototype, by providing a collection of element values for the even-degree prototype, which realize a wide range of passband delay and stopband amplitude responses.

II. TABLES OF ELEMENT VALUES

Five tables containing the element values of even-degree networks up to degree $N=20$ are presented. The notation for the element values as used in the tables is consistent with the notation of Fig. 1. The prototype networks have equiripple passband amplitude and constant group delay in the least squares sense over a percentage of the passband ranging from 50 to 90 percent. All the prototypes have passband insertion loss ripple $R=0.01$ dB and cutoff frequency $\omega_c=1.0$ rad/s at the 0.01-dB point. The choice of $R=0.01$ was a compromise between the conflicting demands of high stopband amplitude selectivity and low passband deviation from constant delay. The tables are classified according to the number of transmission zeros at infinite frequency NZ_∞ and the passband frequency to which the group delay is constant in the least squares sense ω_d. The following combinations

TABLE IV
ELEMENT VALUES FOR LOW-PASS PROTOTYPE
$R=0.01$, $\omega_c=1.0$, $NZ_\infty=8$, $\omega_d=0.6$

R = 0.01 db ω_c = 1.0 rad/sec NZ_∞ = 8 ω_d = 0.6 rad/sec						
N	10	12	14	16	18	20
C1	0.815621	0.821086	0.824939	0.828085	0.830381	0.831966
K1	0.000000	0.000000	0.000000	0.000000	0.000000	0.000000
C2	1.429265	1.439654	1.446863	1.452698	1.456914	1.459804
K2	0.000000	0.000000	0.000000	0.000000	0.000000	0.000000
C3	1.807619	1.823137	1.833560	1.841850	1.847711	1.851678
K3	0.000000	0.000000	0.000000	0.000000	0.000000	0.000000
C4	1.716487	1.735610	1.747817	1.757241	1.763689	1.767958
K4	0.252019	0.084400	0.031689	0.011412	0.004494	0.002325
C5	2.057378	1.958343	1.963323	1.974899	1.983491	1.989127
K5	0.829754	0.406959	0.194547	0.079766	0.034779	0.017516
C6		2.265947	1.861235	1.823996	1.822476	1.827006
K6		0.641823	0.399372	0.232540	0.119573	0.065872
C7			3.046927	2.224089	2.063331	2.035379
K7			0.618130	0.429963	0.294102	0.186373
C8				3.176786	2.202032	1.962083
K8				0.503975	0.366568	0.281454
C9					3.898437	2.681820
K9					0.496217	0.362676
C10						3.889211
K10						0.399137
Average delay(sec)	8.39	11.77	14.64	17.39	20.15	23.03
Delay error(sec)	<0.2	<0.05	<0.05	<0.05	<0.05	<0.05
Phase error(deg)	<0.4	<0.1	<0.1	<0.1	<0.1	<0.2

TABLE V
ELEMENT VALUES FOR LOW-PASS PROTOTYPE
$R=0.01$, $\omega_c=1.0$, $NZ_\infty=10$, $\omega_d=0.5$

R = 0.01 db ω_c = 1.0 rad/sec NZ_∞ = 10 ω_d = 0.5 rad/sec					
N	12	14	16	18	20
C1	0.824024	0.827130	0.829520	0.831626	0.833130
K1	0.000000	0.000000	0.000000	0.000000	0.000000
C2	1.445173	1.451031	1.455343	1.459190	1.461919
K2	0.000000	0.000000	0.000000	0.000000	0.000000
C3	1.831196	1.839522	1.845556	1.850840	1.854557
K3	0.000000	0.000000	0.000000	0.000000	0.000000
C4	1.745202	1.754683	1.761371	1.767094	1.771028
K4	0.000000	0.000000	0.000000	0.000000	0.000000
C5	1.957513	1.971125	1.980378	1.988029	1.993135
K5	0.220769	0.095260	0.034742	0.011984	0.004765
C6	1.937774	1.820416	1.818408	1.825416	1.830880
K6	0.746256	0.393902	0.185040	0.070892	0.031600
C7		2.509630	2.113059	2.033330	2.029260
K7		0.698175	0.451837	0.257340	0.131426
C8			2.907529	2.044965	1.892624
K8			0.553175	0.398118	0.271346
C9				3.603006	2.456524
K9				0.552957	0.409690
C10					3.652247
K10					0.447318
Average delay(sec)	11.02	13.94	16.93	19.59	22.38
Delay error(sec)	<0.1	<0.1	<0.1	<0.1	<0.1
Phase error(deg)	<0.1	<0.1	<0.1	<0.1	<0.1

of NZ_∞ and ω_d are tabulated: $NZ_\infty=2$ and $\omega_d=0.9$ (Table I); $NZ_\infty=4$ and $\omega_d=0.8$ (Table II); $NZ_\infty=6$ and $\omega_d=0.7$ (Table III); $NZ_\infty=8$ and $\omega_d=0.6$ (Table IV); and $NZ_\infty=10$ and $\omega_d=0.5$ (Table V). The value of ω_d associated with each choice of NZ_∞ was found by trial and error to be close to the largest value for a particular table which would not allow the maximum-phase deviation from linearity to exceed 0.5 degrees or the maximum group delay deviation from constant to exceed 0.2. The maximum phase and delay errors for each network are tabulated. Plots of the passband group delay and stopband insertion loss versus frequency for each network, accompany the tables to facilitate selection of a prototype.

The tables were generated as follows. The approximation problem was solved using the Chebyshev rational

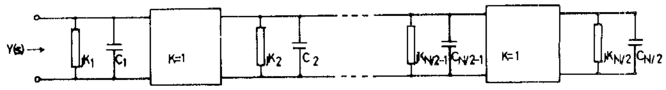

Fig. 2. The even-mode ladder network with input admittance $Y(s)$.

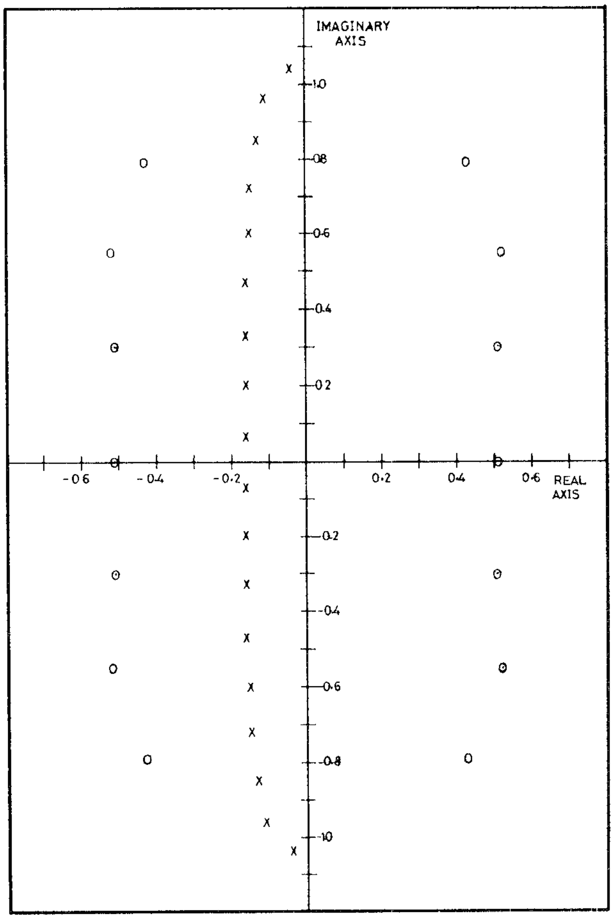

Fig. 3. The pole-zero diagram for the case $R=0.01$ dB, $\omega_c=1.0$, $NZ_\infty=4$, $\omega_d=0.8$, and $N=18$.

function and numerical optimization [9]–[11]. The least squares error criterion was used in the optimization process. As pointed out by Schmidt [12], the least squares criterion is expected to be a practical compromise between the maximally flat and equiripple responses. A detailed examination of the group delay errors of the tabulated networks revealed a tendency towards equiripple behavior over most of the band $0 \leqslant \omega \leqslant \omega d$, associated with the expected increase in error at the edge of the band. The poles of the optimized transfer function were used directly to construct [11] the even-mode admittance function $Y(s)$ of the low-pass prototype, and the network element values were synthesized from $Y(s)$ [1], [7]. The even-mode network is shown in Fig. 2.

The tabulated prototypes are restricted to the even-degree case because of practical problems which arise in the implementation of odd-degree microwave filters [2], [3]. Note that Levy [4] deals with the odd-degree case for one cross-coupling path by making use of an asymmetrical structure.

In order to be realizable by the symmetrical even-degree low-pass prototype network as seen in Fig. 1, the transfer function numerator must be an even polynomial in the complex frequency variable s. This condition constrains finite real or σ axis zeros to occur in pairs with symmetry about the imaginary or $j\ \omega$ axis, finite imaginary axis zeros to occur in pairs with symmetry about the real axis, and finite complex plane zeros to occur with quadrantal symmetry. The finite zeros of the tabulated networks are restricted to zeros with quadrantal symmetry and σ axis zeros. In other words, none of the networks have amplitude responses with finite transmission zeros at real frequencies. Stopband amplitude selectivity is achieved by placing an even number of zeros at infinity.

The pole-zero diagram shown in Fig. 3 serves as an example. The transfer function has degree $N=18$, the number of zeros at infinity $NZ_\infty=4$, passband ripple level $R=0.01$ dB and group delay constant, in the least squares sense, to $\omega_d=0.9$ rad/s. There are 14 finite zeros consisting of one pair on the real axis and three sets with quadrantal symmetry.

Restriction of the transmission zeros to infinity makes the prototypes suitable for the design of generalized interdigital filters [2], as finite transmission zeros cannot be realized in this structure. The prototypes can obviously also be used for the design of generalized direct-coupled cavity waveguide filters [3]–[5] and generalized combline filters [6].

III. Analysis of the Networks

The response plots (see Figs. 4–8) which accompany the tables might be found to contain insufficient information. For example, an expanded scale group delay or phase deviation plot, or the stopband insertion loss beyond $\omega=2$ rad/s, may be required. In the latter case, the plots may be extrapolated quite accurately beyond $\omega=2$ by increasing the insertion loss by 6 NZ_∞ dB/octave.

The necessary information can be obtained by making use of a simple algorithm for computing the amplitude, phase, or group delay of the low-pass prototype with known element values. The algorithm is described below.

Due to the symmetry of the prototype network in Fig. 1, the transfer function $t(s)$ can be written in terms of the even- and odd-mode admittances $Y(s)$ and $Y^*(s)$ as [1]

$$t(s)=\frac{Y(s)-Y^*(s)}{[1+Y(s)][1+Y^*(s)]} \tag{1}$$

if the terminating resistors are unity. The even- and odd-mode networks are simple ladder networks containing lumped capacitances, frequency independent susceptances, and unity admittance inverters. Fig. 2 shows the degree $N/2$ even-mode network for the degree N prototype of Fig. 1. The odd-mode admittance $Y^*(s)$ is obtained by replacing the complex coefficients of the numerator and denominator polynomials of $Y(s)$ by their complex conjugates.

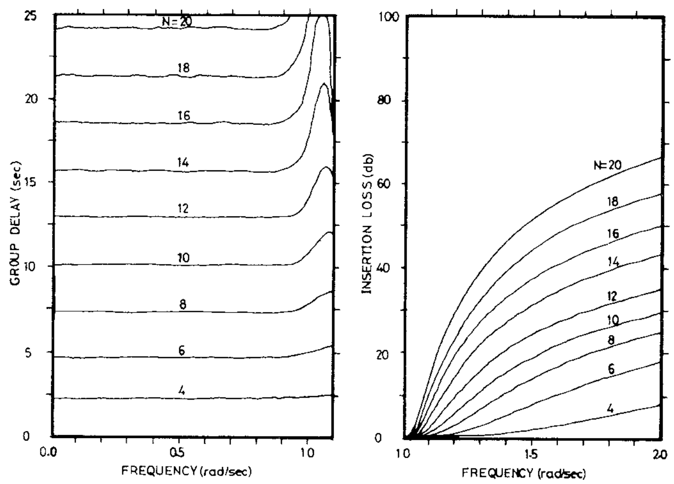

Fig. 4. Passband group delay and stopband insertion loss for Table I: $R=0.01$ dB, $\omega_c=1.0$, $NZ_\infty=2$, $\omega_d=0.9$.

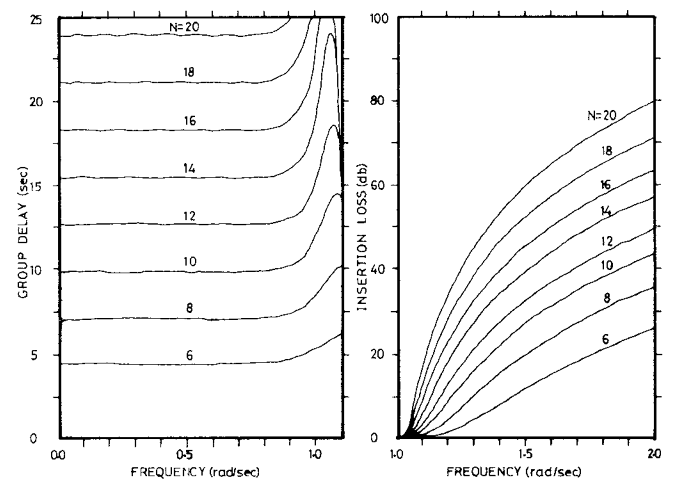

Fig. 5. Passband group delay and stopband insertion loss for Table II: $R=0.01$ dB, $\omega_c=1.0$, $NZ_\infty=4$, and $\omega_d=0.8$.

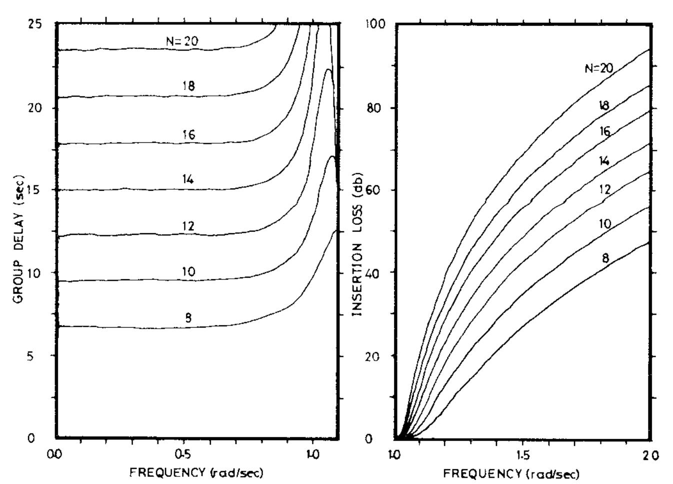

Fig. 6. Passband group delay and stopband insertion loss for Table III: $R=0.01$ dB, $\omega_c=1.0$, $NZ_\infty=6$, and $\omega_d=0.7$.

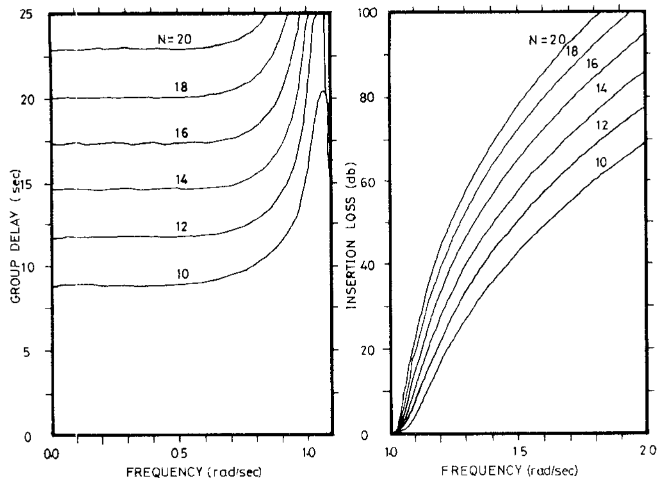

Fig. 7. Passband group delay and stopband insertion loss for Table IV: $R=0.01$ dB, $\omega_c=1.0$, $NZ_\infty=8$, and $\omega_d=0.6$.

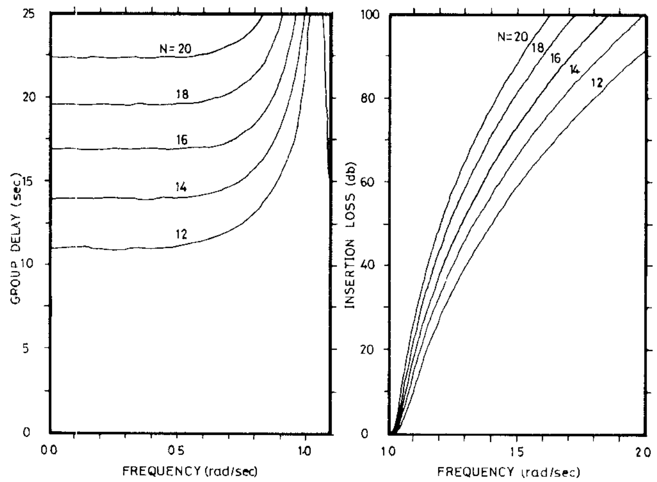

Fig. 8. Passband group delay and stopband insertion loss for Table V $R=0.01$ dB, $\omega_c=1.0$, $NZ_\infty=10$, and $\omega_d=0.5$.

Let

$$Y(s)|_{s=j\omega}=jA(\omega) \tag{2}$$

$$Y^*(s)|_{s=j\omega}=jB(\omega). \tag{3}$$

By substitution of (2) and (3) in (1) and manipulation, the magnitude squared function $|t(\omega)|^2$, the phase function $\phi(\omega)$, and the group delay function $D(\omega)$ are found to be

$$|t(\omega)|^2=\frac{[A(\omega)-B(\omega)]^2}{[1+A^2(\omega)][1+B^2(\omega)]} \tag{4}$$

$$\phi(\omega)=-\tan^{-1}\left[\frac{1-A(\omega)B(\omega)}{A(\omega)+B(\omega)}\right] \tag{5}$$

$$D(\omega)=\frac{\frac{\partial A(\omega)}{\partial\omega}}{1+A^2(\omega)}+\frac{\frac{\partial B(\omega)}{\partial\omega}}{1+B^2(\omega)}. \tag{6}$$

The functions $A(\omega)$, $B(\omega)$, $\Delta(\omega)=A(\omega)-B(\omega)$, $A'(\omega)=\partial A(\omega)/\partial\omega$, and $B'(\omega)=\partial B(\omega)/\partial\omega$ may be evaluated by the following recurrence equations. To avoid roundoff errors for values of $\omega>1$ the difference between $A(\omega)$ and $B(\omega)$, $\Delta(\omega)$ should be evaluated recursively as shown.

$$\left.\begin{aligned} A_i&=\omega C_i+K_i-\frac{1}{A_{i+1}}\\ B_i&=\omega C_i-K_i-\frac{1}{B_{i+1}}\\ \Delta_i&=2K_i+\frac{\Delta_{i+1}}{A_{i+1}B_{i+1}}\\ A_i'&=C_i+\frac{A_{i+1}'}{A_{i+1}^2}\\ B_i'&=C_i+\frac{B_{i+1}'}{B_{i+1}^2}\end{aligned}\right\}, \quad \text{for} \quad i=N/2-1,\cdots,2,1 \tag{7}$$

with initial values

$$\begin{aligned} A_{N/2}&=\omega C_{N/2}+K_{N/2}\\ B_{N/2}&=\omega C_{N/2}-K_{N/2}\\ \Delta_{N/2}&=2K_{N/2}\\ A_{N/2}'&=C_{N/2}\\ B_{N/2}'&=C_{N/2}.\end{aligned} \tag{8}$$

The notation used in these equations is consistent with Fig. 2. The elements C_1, K_1 are at the port of the network.

The network functions are evaluated at the frequency ω by using $A(\omega)=A_1$, $B(\omega)=B_1$, $\Delta(\omega)=\Delta_1$, $A'(\omega)=A_1'$, and $B'(\omega)=B_1'$ in (4)–(6).

IV. Conclusions

The element values of a collection of low-pass nonminimum-phase networks have been tabulated. The networks may be used as prototypes for the design of narrow-band bandpass microwave linear-phase filters using the generalized interdigital, generalized direct-coupled cavity waveguide, and generalized combline structures. For a wide range of amplitude and phase specifications, the tabulated networks eliminate the need for computer programs to solve the low-pass approximation and synthesis problems.

Acknowledgment

The author wishes to thank Dr. J. A. G. Malherbe, who suggested the compilation of a set of tables of nonminimum-phase low-pass prototypes, Prof. H. C. Viljoen, Prof. J. J. du Plessis, and P. W. van der Walt, all of the Department of Electrical Engineering, University of Stellenbosch, South Africa, for assistance and support. He is also indebted to Dr. T. J. Hugo, the Director of the National Institute for Aeronautics and Systems Technology of the South African Council for Scientific and Industrial Research for support.

References

[1] J. D. Rhodes, "A lowpass prototype network for microwave linear phase filters," *IEEE Trans. Microwave Theory Tech.*, vol. MTT-18, pp. 290–301, June 1970.

[2] ——, "The generalized interdigital linear phase filter," *IEEE Trans. Microwave Theory Tech.*, vol. MTT-18, pp. 301–307, June 1970.

[3] ——, "The generalized direct-coupled cavity linear-phase filter," *IEEE Trans. Microwave Theory Tech.*, vol. MTT-18, pp. 308–313, June 1970.

[4] R. Levy, "Filters with single transmission zeros at real or imaginary frequencies," *IEEE Trans. Microwave Theory Tech.*, vol. MTT-24, pp. 172–181, Apr. 1976.

[5] A. E. Atia and A. E. Williams, "Nonminimum-phase optimum-amplitude bandpass waveguide filters," *IEEE Trans. Microwave Theory Tech.*, vol. MTT-22, pp. 425–431, Apr. 1974.

[6] R. Levy, "Mixed lumped and distributed linear phase filters," in *1974 European Conf. on Circuit Theory and Design*, IEE (London), Conf. Publ. no. 116, pp. 32–37.

[7] J. D. Rhodes, "Filters with periodic phase delay and insertion-loss ripple," in *Proc. Inst. Elec. Eng.*, vol. 119, no. 1, pp. 28–32, Jan. 1972.

[8] ——, "Filters approximating ideal amplitude and arbitrary phase characteristics," *IEEE Trans. Circuit Theory*, vol. CT-20, pp. 120–124, Mar. 1973.

[9] R. J. Wenzel, "Solving the approximation problem for narrowband bandpass filters with equal-ripple passband response and arbitrary phase response," in *1975 IEEE MTT-S Int. Microwave Symp.*, IEEE Catalog no. 75CH0955-5, p. 50.

[10] Von K. Wittman, G. Pfitzenmaier, and F. Künemund, "Dimensionierung reflexionsfaktor-und laufzeitgeebneter versteilerter Filter mit Überbrückungen," *Frequenz*, vol. 24, pp. 307–312, Oct. 1970.

[11] J. H. Cloete, "Microwave linear phase filters," Progress report no. 2, Dept. Electrical Engineering, Univ. Stellenbosch, South Africa, Feb. 1978. (Copies may be obtained from the Head of the Department.)

[12] C. E. Schmidt, "Delay equalizers," *Wescon Digest*, Los Angeles, CA, Aug. 1970.

Band-Limited Deconvolution of Locating Reflectometer Results

PETER I. SOMLO, SENIOR MEMBER, IEEE

***Abstract*—The locating reflectometer [1] is a frequency-swept microwave instrument which, by analog Fourier transformation, converts the reflection coefficient, a function of frequency $\Gamma(s)$, into the spatial distribution of the reflection coefficient $\Gamma(x)$. It will be shown that by the method of deconvolution an increase in axial resolution may result. By making use of the fact that the real and imaginary parts of the "locating plot" $\Gamma(x)$ are a Hilbert transform pair, a signal-to-noise ratio improvement is achieved by averaging the results of complex deconvolution using only the real and then only the imaginary parts of the locating plots. A number of experimental results are given, illustrating the increase in axial resolution when the method of band-limited deconvolution is applied to some typical waveguide components and obstacles.**

I. Formulation of the Problem

LET US assume that we have an instrument, a locating reflectometer[1] (LR) [1], that gives a plot of the distribution of the (complex) reflection coefficient $h(x)$ of a component having a number of internal reflections as a function of distance along the waveguide x. This distribution will be referred to as the "locating vector." Assume that, if more than one reflection is present in the waveguide tested, the instrument will record the *superposition* of these reflections. Because of the bandwidth limitation of the instrument, the locating plot of a single lumped reflection will have some axial spread, since zero spread would require infinite bandwidth. This response to a single lumped reflection we shall call the "instrument function" $g(x)$ which some other workers have referred to as the "pulse response" or the "aperture function." Since we have assumed that the instrument superimposes individual lumped reflection coefficient plots of axial distributions

$$h(x)=\sum_{i=1}^{k}\left[a_i g(x-x_i)\right] \tag{1}$$

i.e., k individual reflection coefficient axial distributions with different complex magnitudes and central positions are added to form the observed locating vector $h(x)$. In other words, we may regard $h(x)$ as the sum of a number of scaled and shifted identical functions. It is well known [2] that the convolution of a function with an impulse function (Dirac function) will duplicate the given function, and, similarly, the convolution of a given function with a number of weighted and shifted impulse functions will produce the sum of the weighted and shifted original functions. Designating the set of weighted and shifted impulse functions as $f(x)$, the observed locating vector is

Manuscript received April 10, 1978; revised July 6, 1978.

The author is with the National Measurement Laboratory, CSIRO, Sydney, Australia 2070.

[1] The locating reflectometer grew out of two reflectometers, the high resolution reflectometer [7] and the comparison reflectometer [8], resulting in an analog instrument with the minimum of electronic circuitry but yielding the values and the locations of individual reflections.

0018-9480/79/0200-0128$00.75